Context-specific striatal astrocyte molecular responses are phenotypically exploitable

Xinzhu Yu, Jun Nagai, Maria Marti-Solano, Joselyn S. Soto, Giovanni Coppola, M. Madan Babu & Baljit S. Khakh

Correspondence to: bkhakh@mednet.ucla.edu

Supplemental information

Table S1.

Figures S1-S6.

Excel File S1: Data reporting the IP DEGs (FDR < 0.05, FPKM > 1) for all the astrocyte-specific RNA-seq projects (related to Figure 1).

Excel File S2: Data reporting genes that belong to each of the WGCNA modules (related to Figure 1).

Excel File S3: Data reporting statistical analyses, n numbers and relevant parameters (related to Figures 3-5, 7 and Figure S6).

Excel File S4: Data reporting raw replicate values (related to Figures 3-5, 7 and Figure S6).

Excel File S5: Data reporting the GPCRs identified from RNA-seq of NCAR and R6/2 (related to Figure 8).

Table S1. Summary of astrocyte-specific RNA-sequencing data for validated experimental perturbations (related to Figure 1).

	Experimental perturbations	Groups	§Accession number	Age	Number of mice	Validation	References
Huntington's disease	R6/2 mice	NCAR	GSE124846	1 month	4	*IHC	(Diaz-Castro et al., 2019)
		R6/2			4		
		NCAR		2 months	4		
		R6/2			4		
		NCAR		3 months	4		
		R6/2			4		
	Q175 mice	WT		2 months	4		
		Q175			4		
		WT		12 months	4		
		Q175			4		
Pathology	Ablation of medium spiny neurons	Vehicle	GSE143475	9 weeks	4	#IHC	Figure S2 in current paper
		QA			4		
	Neuroinflammation	Vehicle		9 weeks	4	#Behavior	Figure S2 in current paper
		LPS			4		
	Ablation of dopaminergic neurons	Vehicle	GSE153791	9 weeks	4	#IHC	Figure S2 in current paper
		MPTP			4		
	Obsessive-compulsive disorder-like mouse model	WT	GSE153791	5 months	4	#IHC, #Behavior	Figure S2 in current paper
		SAPAP3 KO			4		
Ionic signaling	K^+ current reduction	Kir4.1$^{flox/flox}$ + Control AAV	GSE143475	9 weeks	4	#IHC	Figure S2 in current paper
		Kir4.1$^{flox/flox}$ + Cre AAV			4		
	Ca^{2+} signaling attenuation	Control AAV	GSE114757	9 weeks	4	*IHC, *Ca^{2+} imaging, *behavior	(Yu et al., 2018)
		CalEx AAV			4		
		WT	GSE143475	9 weeks	4	*Ca^{2+} imaging	(Yu et al., 2018)
		IP_3R2 KO			4		
GPCR signaling	Gq activation	hM3Dq + Vehicle		9 weeks	4	#IHC, *Ca^{2+} imaging	(Chai et al., 2017) Figure S2 in current paper
		hM3Dq + CNO			4		
	Gi activation	hM4Di + Vehicle	GSE119058	9 weeks	4		

		hM4Di + CNO			4	*#IHC, *Ca^{2+} imaging, *behavior	(Chai et al., 2017; Nagai et al., 2019) Figure S2 in current paper
	Gs activation	rM3Ds + Vehicle	GSE143475	9 weeks	4	#IHC, *Ca^{2+} imaging	(Chai et al., 2017) Figure S2 in current paper
		rM3Ds + CNO			4		

Abbreviations: NCAR – Non-carrier; WT – Wild-type; QA – Quinolinic acid; MPTP – 1-methyl-4-phenyl-1,2,3,6-tetrahydropyridine); KO – Knockout; IHC – Immunohistochemistry

§ Data deposited in the Gene Expression Omnibus (GEO) repository (https://www.ncbi.nlm.nih.gov/geo) * Validation previously published by us. # Validation data reported in current paper

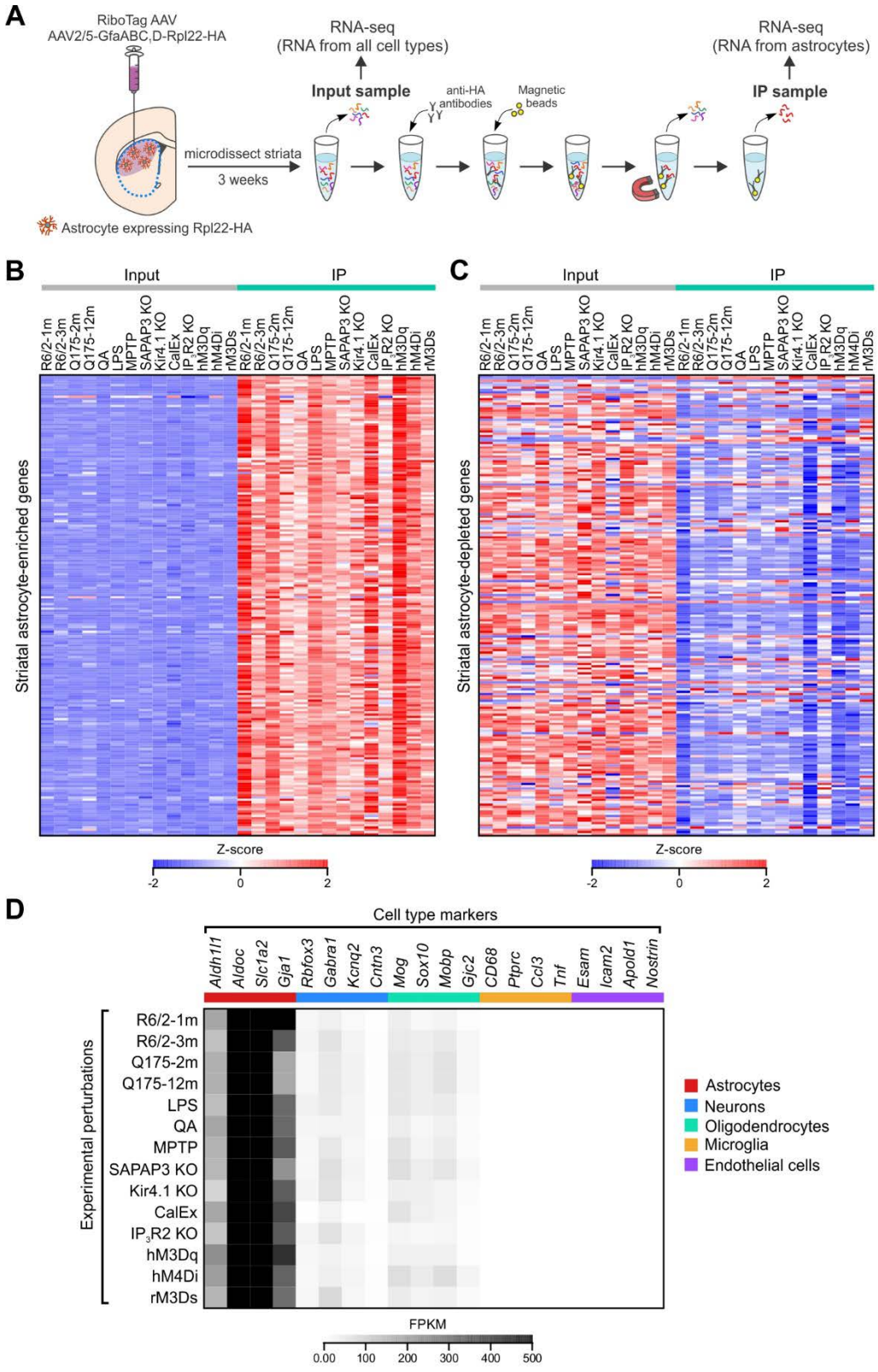
A
RiboTag AAV
AAV2/5-GfaABC1D-Rpl22-HA
RNA-seq
(RNA from all cell types)
Input sample
anti-HA
antibodies
Magnetic
beads
RNA-seq
(RNA from astrocytes)
IP sample
microdissect striata
3 weeks
Astrocyte expressing Rpl22-HA
B
Input
IP
R6/2-1m
R6/2-3m
Q175-2m
Q175-12m
QA
LPS
MPTP
SAPAP3 KO
Kir4.1 KO
CalEx
IP3R2 KO
hM3Dq
hM4Di
rM3Ds
Striatal astrocyte-enriched genes
Z-score
-2
0
2
C
Striatal astrocyte-depleted genes
D
Cell type markers
Aldh1l1
Aldoc
Slc1a2
Gja1
Rbfox3
Gabra1
Kcnq2
Cntn3
Mog
Sox10
Mobp
Gjc2
CD68
Ptprc
Ccl3
Tnf
Esam
Icam2
Apold1
Nostrin
Experimental perturbations
Astrocytes
Neurons
Oligodendrocytes
Microglia
Endothelial cells
FPKM
0.00
100
200
300
400
500

Figure S1: Astrocyte-enriched genes are highly expressed in striatal IP RNA samples across 14 experimental perturbations (EPs) (related to Figure 1). (**A**) Schematic of experimental design and RNA extraction procedure. RiboTag AAV was microinjected into dorsal striatum 3 weeks before RNA extraction. Astrocyte RNA was immunoprecipitated using specific anti-HA antibodies. Input samples contain RNA from all cell types in the striatum while IP samples contain RNA from astrocytes. (**B**) The heatmap showing relative expression levels of top 200 striatal astrocyte-enriched genes in both input and IP samples of 14 EPs. (**C**) The heatmap showing relative expression levels of top 200 striatal astrocyte-depleted genes in both input and IP samples. (**D**) The heatmap showing FPKM levels of marker genes for astrocytes, neurons, oligodendrocytes, microglia and endothelial cells in corresponding control IP samples of 14 EPs.

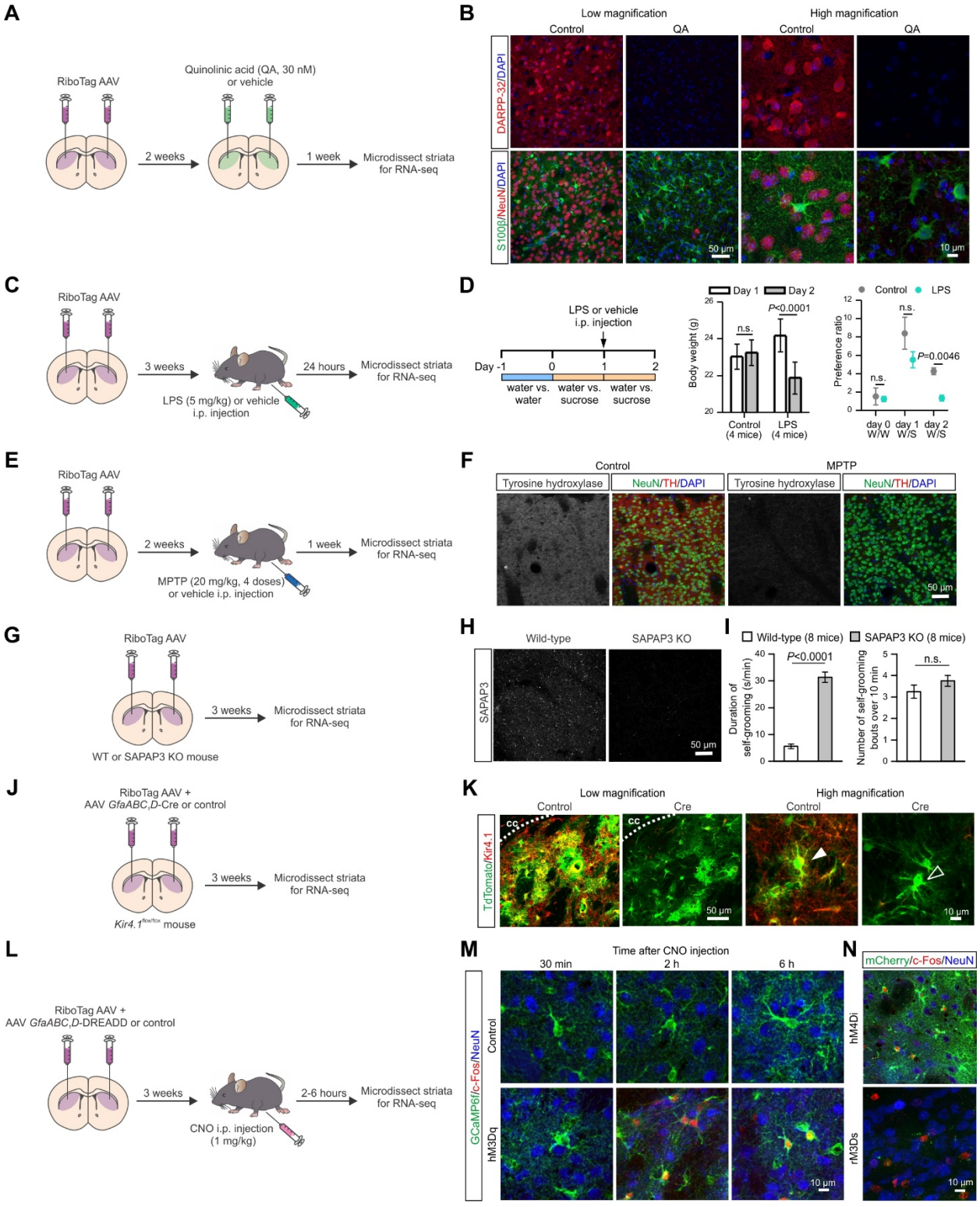

Figure S2: Validation of EPs with immunohistochemistry and behavior (related to Figure 1). (**A**) Schematic of experimental design of medium spiny neuron (MSN) ablation with Quinolinic acid (QA). RiboTag AAV was microinjected into dorsal striatum 3 weeks before RNA extraction.

QA (30 nM) or vehicle was microinjected 1 week before RNA extraction. (**B**) Representative immunohistochemistry (IHC) images of the dorsal striatum showing reduction in immunoreactivity of DARPP-32 for MSNs but not S100β for astrocytes. (**C**) Schematic of experimental design to induce neuroinflammation with LPS. RiboTag AAV was microinjected into dorsal striatum 3 weeks before RNA extraction. LPS or vehicle was administered through i.p. injection 24 hours before RNA extraction. (**D**) Both body weight and sucrose preference ratio were significantly decreased 24 hours after LPS injection. Data: mean ± SEM (n = 4 mice). (**E**) Schematic of experimental design of dopaminergic neuron ablation with MPTP. RiboTag AAV was microinjected into dorsal striatum 3 weeks before RNA extraction. MPTP (20 mg/kg body weight) or vehicle was administered through i.p. injection every 2h for a total of 4 doses one week before RNA extraction. (**F**) Representative IHC images showing reduced expression of tyrosine hydroxylase in the dorsolateral striatum by MPTP, indicating the loss of dopaminergic input. (**G**) Schematic of experimental design to exact RNA from striatal astrocytes in SAPAP3 KOs and WT littermate controls by delivering RiboTag AAV into the dorsal striatum 3 weeks before RNA extraction. (**H**) Representative IHC images showing reduced expression of SAPAP3 in the dorsolateral striatum of SAPAP3 KO. (**I**) The duration of self-grooming (left) was significantly longer in SAPAP3 KO compared with WT littermates, while the number of grooming bouts was not different (right). (**J**) Schematic of experimental design to reduced Kir4.1 expression. RiboTag AAV and AAV *GfaABC$_1$D*-Cre or tdTomato was microinjected into dorsal striatum 3 weeks before RNA extraction. (**K**) Representative IHC images showing that Kir4.1 was expressed in dorsal striatal astrocytes in the absence of Cre (indicated by an arrow), but was absent in astrocytes in the presence of Cre (indicated by an open arrow). (**L**) Schematic of experimental design of DREADD activation. AAVs encoding RiboTag and DREADD were microinjected into dorsal striatum 3 weeks before RNA extraction. CNO (1 mg/kg body weight) was administered through i.p. injection 2-6 hours before RNA extraction. (**M**) c-Fos expression increases in striatal astrocytes expressing hM3Dq 2- and 6-hour after CNO injection. (**N**) c-Fos expression increases in striatal astrocytes expressing hM4Di and rM3Ds 2-hour after CNO injection.

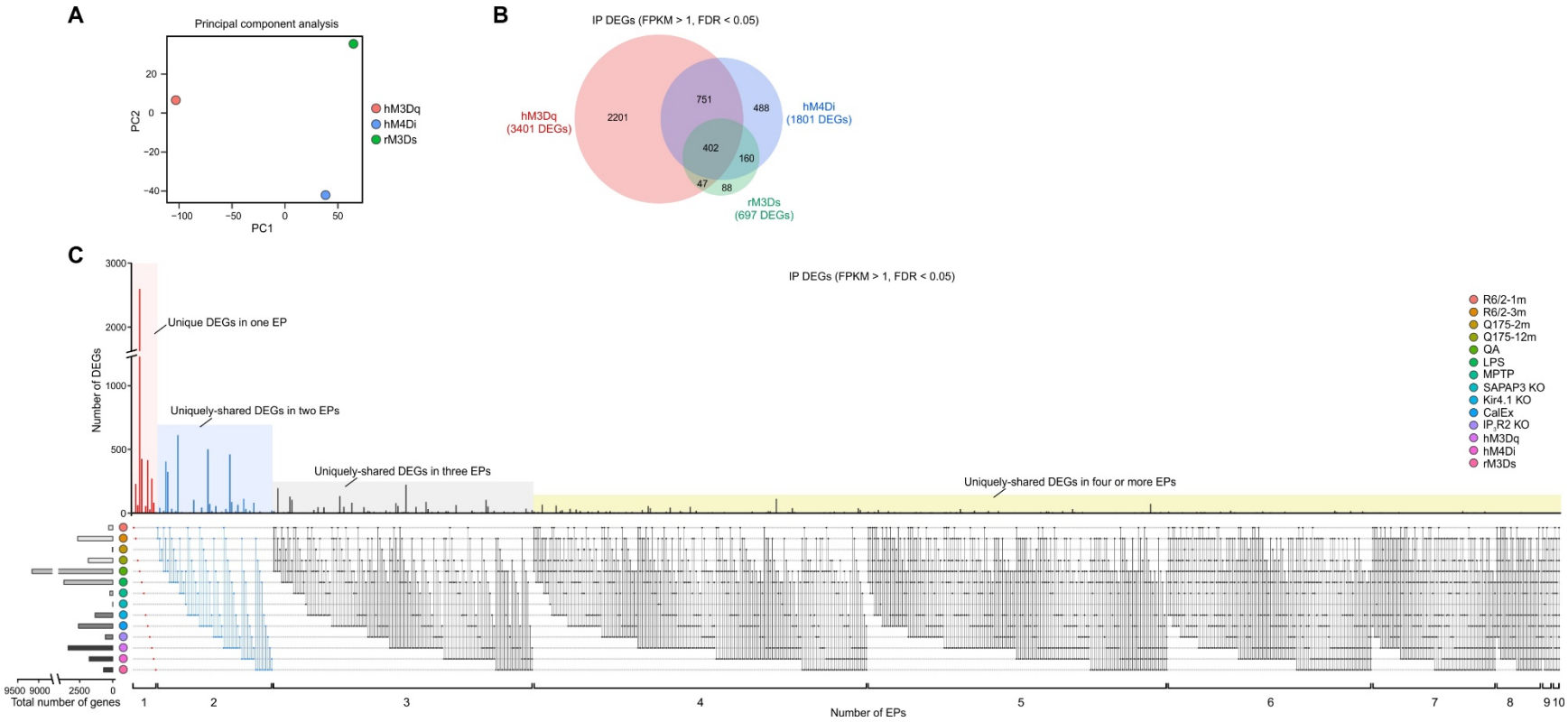

Figure S3: Striatal astrocytes exhibit context-specific gene expression changes under various EPs (related to Figure 1). (**A**) Principal component analysis plot of IP DEGs (FPKM > 1, FDR < 0.05) from three EPs of GPCR activation, including hM3Dq, hM4Di and rM3Ds. (**B**) Venn diagram showing the numbers of DEGs (FPKM > 1, FDR < 0.05) in the IP samples shared by three EPs of GPCR activation. (**C**) UpSet plot showing numbers of unique DEGs (FPKM > 1, FDR < 0.05) shared by 14 EPs. There were zero DEGs shared by more than 10 EPs and therefore nothing is listed in the plot for that.

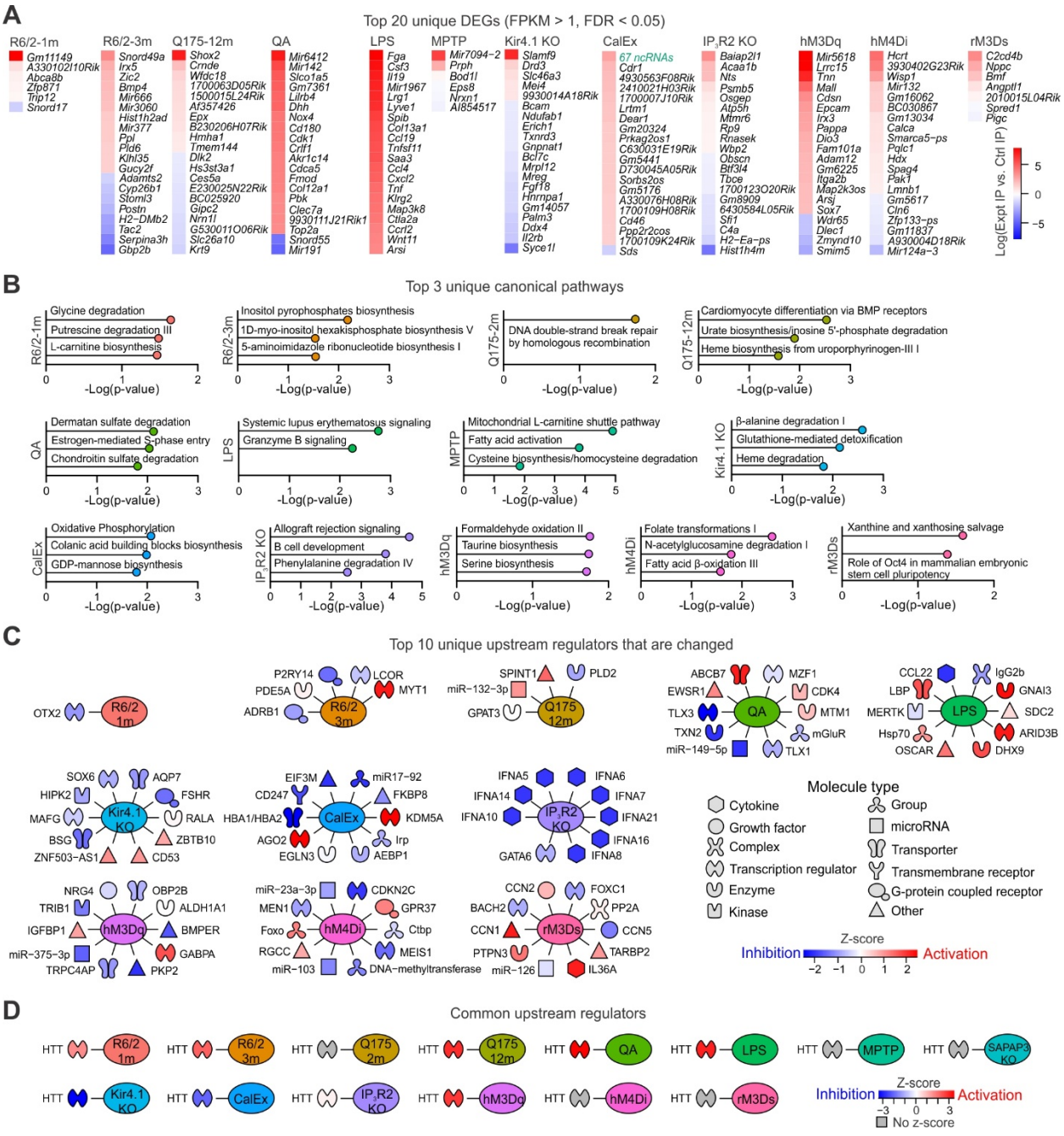

Figure S4: Unique DEGs, canonical pathways and upstream regulators across different EPs (related to Figure 1). (**A**) Heatmaps of the top 20 unique DEGs for each EP. Two EPs including Q175-2m and SAPAP3 KO did not have any unique DEGs and therefore were not listed. (**B**) Top 3 unique canonical pathways of striatal astrocytes, identified by Ingenuity Pathway Analysis (IPA), for each EP ($P < 0.05$). SAPAP3 KO did not have any unique canonical pathways and therefore was not listed. (**C**) Top 10 unique upstream regulators that were significantly associated with each intervention ($P < 0.05$). Shapes represent molecule type and colors indicate regulators either activated (red) or inhibited (blue) based on z-scores. Three EPs including Q175-2m, MPTP and SAPAP3 KO did not have any unique DEGs and therefore were not listed. (**D**) HTT was the

only common upstream regulator that significantly associated with all EPs ($P < 0.05$). HTT showed diverse changes across all EPs that were reflected by z-scores (blue indicates inhibition while red indicates activation of HTT).

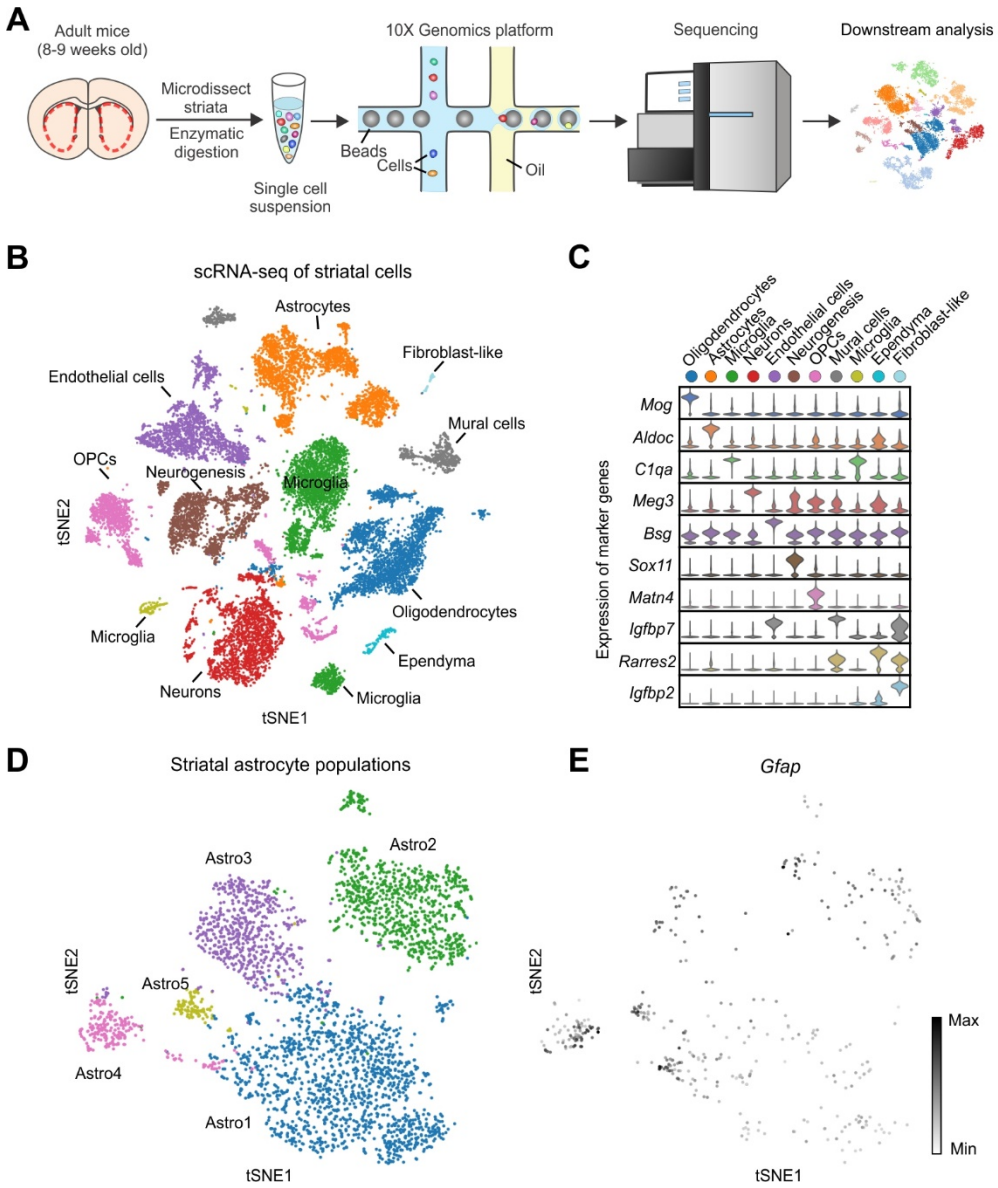

Figure S5: Single cell RNA-sequencing (scRNA-seq) of adult mouse striatum (related to Figure 2). (**A**) Schematic of experimental procedure for scRNA-seq. Single cells were dissociated from the striatum of adult mice (8-9 weeks old) and were processed with 10X Genomics platform. (**B**) *t*-distributed stochastic neighbor embedding (*t*-SNE) plot of 20912 striatal cells grouped by expression similarity identified 11 major cell populations in the mouse striatum. (**C**) Violin plot showing relative expression levels of cell type marker genes for 11 transcriptomic clusters identified in striatal scRNA-seq. (**D**) *t*-SNE plot of 3244 striatal astrocytes identified 5 astrocyte subpopulations. (**E**) Astrocyte gene *Gfap* had relatively low expression levels across striatal astrocytes and therefore was not identified as a marker gene for any astrocyte subpopulations.

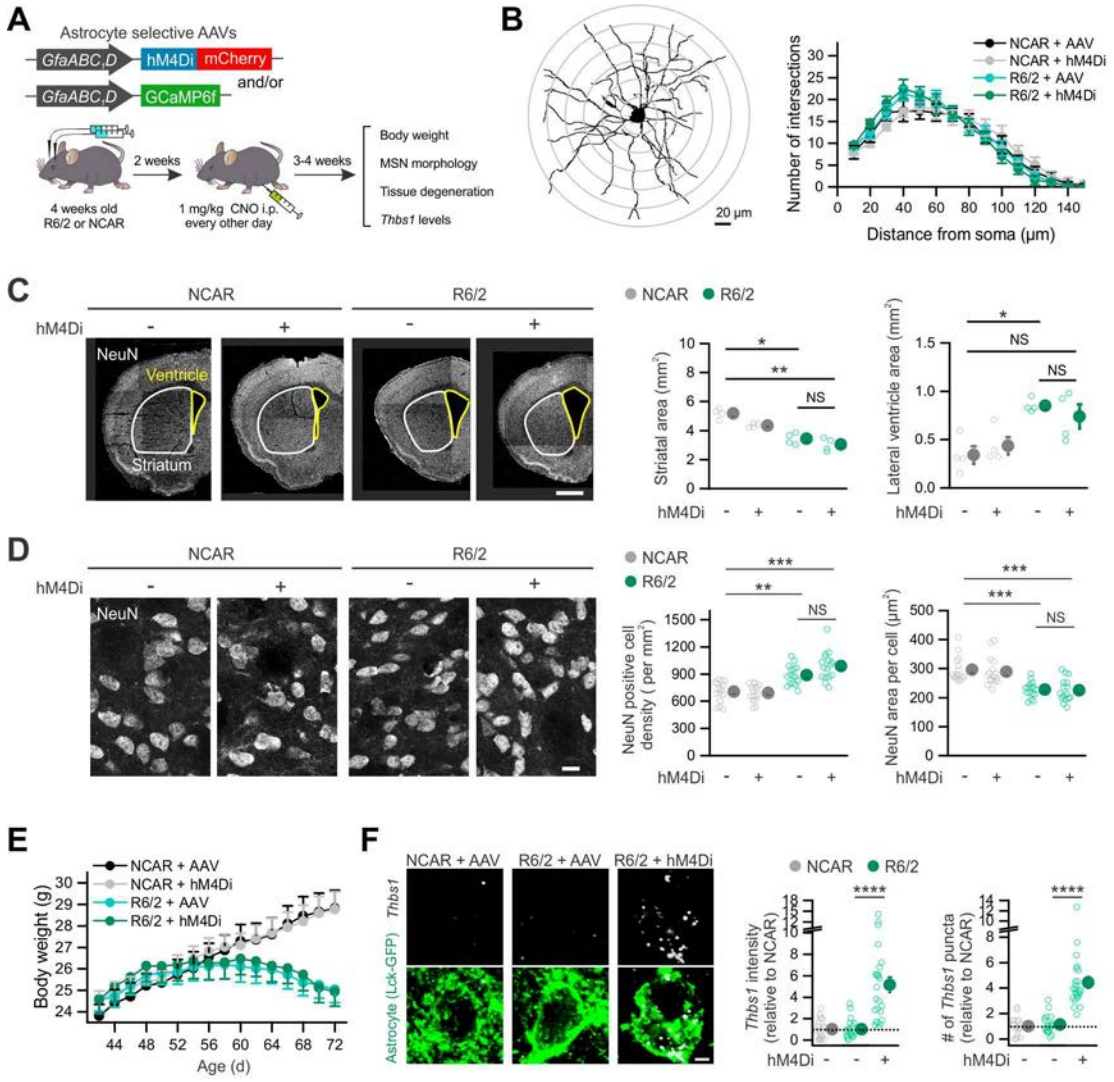

Figure S6: Gi-GPCR pathway activation in striatal astrocytes increased *Thbs1* mRNA expression in HD mice (related to Figures 4 and 5). (**A**) Schematic of experimental design. AAV was microinjected into the dorsal striatum when mice were 4 weeks old and CNO was injected every 2 days from 6 weeks old for 3-4 weeks before experimental assessments. (**B**) Sholl analysis of MSN morphology revealed no significant difference of branching patterns among indicated four experimental groups (n = 6-7 MSNs from 4 mice per group). (**C**) The R6/2 + AAV group showed the reduction in size of the striatum and the increase in size of the lateral ventricle (LV) compared to the NCAR + AAV group (P = 0.04). Astrocyte G_i-GPCR activation did not alter the tissue degeneration (P > 0.99). Stereological analysis for tissue volume (see STAR Methods) further confirmed the results by estimating the volume of the striatum (7.9 ± 0.4 in NCAR + AAV; 7.0 ± 0.1 in NCAR + hM4Di; 5.1 ± 0.4 in R6/2 + AAV; 4.7 ± 0.2 in R6/2 + hM4Di [mm^3]) and LV (0.8 ± 0.2 in NCAR + AAV; 1.0 ± 0.1 in NCAR + hM4Di; 1.3 ± 0.1 in R6/2 + AAV; 1.2 ± 0.2 in R6/2 + hM4Di [mm^3]). (**D**) The R6/2 + AAV group showed increased density and decreased size of NeuN positive neurons when compared to the NCAR + AAV group (16 FOVs from 4 mice per group, P < 0.0054) and these changes were not affected by hM4Di stimulation in R6/2 mice (P > 0.99). (**E**) Mean body weights of mice. R6/2 mice showed the expected reduction in body weight with ageing. hM4Di activation in dorsal striatal astrocytes did not affect body weights in R6/2 (*P*

= 0.14, two-way ANOVA repeated measures, 19 mice for R6/2 + AAV, 20 mice for R6/2 + hM4Di) or NCAR mice (P = 0.13, two-way ANOVA repeated measures, 19 mice for NCAR + AAV, 19 mice for NCAR + hM4Di). (**F**) RNAscope based fluorescent *in situ* hybridization assessment of *Thbs1* mRNA expression in the dorsal striatum of the three experimental groups (n = 20-24 astrocytes from 4 mice per group). IHC for virally delivered Lck-GFP in astrocytes was performed to demarcate astrocytes that received viruses. Significant upregulation of *Thbs1* mRNA was observed in the R6/2 + hM4Di group. Scale bars: 1 mm in **C**, 20 µm in **D** and 1 µm in **E**. Data are shown as mean ± SEM. *P < 0.05, **P < 0.01, ***P < 0.001, ****P < 0.0001. Full details of n numbers, precise P values, statistical tests and the raw values are reported in **Excel files S3** and **S4**.